IOPscience iopscience.iop.org

Home Search Collections Journals About Contact us My IOPscience

Optical and Raman correlation of laser recrystallised and quenched amorphous silicon film: a microprobe study

This content has been downloaded from IOPscience. Please scroll down to see the full text.

1990 J. Phys. D: Appl. Phys. 23 729

(http://iopscience.iop.org/0022-3727/23/6/016)

View the table of contents for this issue, or go to the journal homepage for more

Download details:

IP Address: 140.113.38.11
This content was downloaded on 28/04/2014 at 19:45

Please note that terms and conditions apply.

J. Phys. D: Appl. Phys. 23 (1990) 729–734. Printed in the UK

Optical and Raman correlation of laser recrystallised and quenched amorphous silicon film: a microprobe study

C R Huang†, M C Lee‡, Y S Chang§, C C Lin‡ and Y F Chao‡

† Mechanical Industry Research Laboratory of ITRI, Department of Laser Technology, Building 22, 195 Chung Hsing Road, Section 4 Chutung, Hsinchu, Taiwan 31015, Republic of China
‡ Department of Electrophysics and Institute of Electro-optical Engineering, National Chiao Tung University, Hsinchu, Taiwan 30049, Republic of China
§ Electronics Research and Service Organization of ITRI, Display Technology Group, Building 11, 195 Chung Hsing Road, Section 4 Chutung, Hsinchu, Taiwan 31015, Republic of China

Received 3 October 1989, in final form 10 January 1990

Abstract. The amorphous silicon film, excited by a picosecond laser, has been investigated by a laser microprobe. The optical properties are measured simultaneously with its Raman spectrum. The sharp Raman peak of this properly annealed film is similar to that of crystalline silicon (c-Si) with a significant drop in reflection. A second pulse of proper fluence can reduce the Raman intensity and increase the transmission greatly and this is ascribed to explosive crystallisation and laser quenching. This reamorphisation phenomenon of the annealed film suggests a feasible method for erasable optical recording.

1. Introduction

In recent years, amorphous silicon (a-Si) has drawn great attention because of its potential applications in fast photoconductors, large panel solar cells, photoreceptors for electrophotographics, and thin film microelectronics [1–4]. Its optical recording capability has been demonstrated [5] and a high contrast in transmission has been achieved by the laser annealing technique [6]. However, its erasability was only briefly studied by laser quenching [7]. Using a microprobe, we study phase variation of the a-Si film after various excitations by a picosecond laser. The Raman intensity and optical signal, which were simultaneously measured by the microprobe, are clearly correlated. This may be ascribed to explosive crystallisation and laser quenching [8–11]. Laser-induced strain [12] is also observable from the recrystallised Raman peak. After two consecutive excitations of proper fluence, the Raman intensity significantly dropped which indicates the annealed Si is re-amorphised. Such a change is also accompanied by a large contrast in reflection and transmission, so that a-Si film could be used for erasable recording.

2. Experimental details

Using the same method as that of Lee *et al* [6], we prepared three samples of a-Si film with different thicknesses (0.8, 1.2 and 1.8 μm) on cover glasses. These films were excited by a nitrogen laser (PRA LN-1000, 800 ps at 337 nm) and a dye laser (PRA LN-107, 600 ps at 580 nm) of various fluences ranging from 0.1 to 1.4 J cm^{-2}. The microstructure of these annealed films was then examined by an optical microscope ($\times$400) and a scanning electron microscope (SEM). The Raman spectrum across the excited region was measured every 5 μm by a CW argon laser microprobe ($\simeq$2 mW, 10 μm at $1/e^2$). Except for strain measurement, a 75 μm entrance slit was used, and all other signals were collected into a double monochromator (Jobin Yvon U-1000) through a 500 μm entrance slit. Because the microprobe merely provides weak scattering signals, a multichannel detector (Princeton Instruments IRY-1024G) was employed to increase the signal-to-noise ratio. The wide spectral range was detected by long time accumulation. The transmission and reflectivity of the film were measured simultaneously by the same microprobe.

0022-3727/90/060729 + 05 $03.50 © 1990 IOP Publishing Ltd

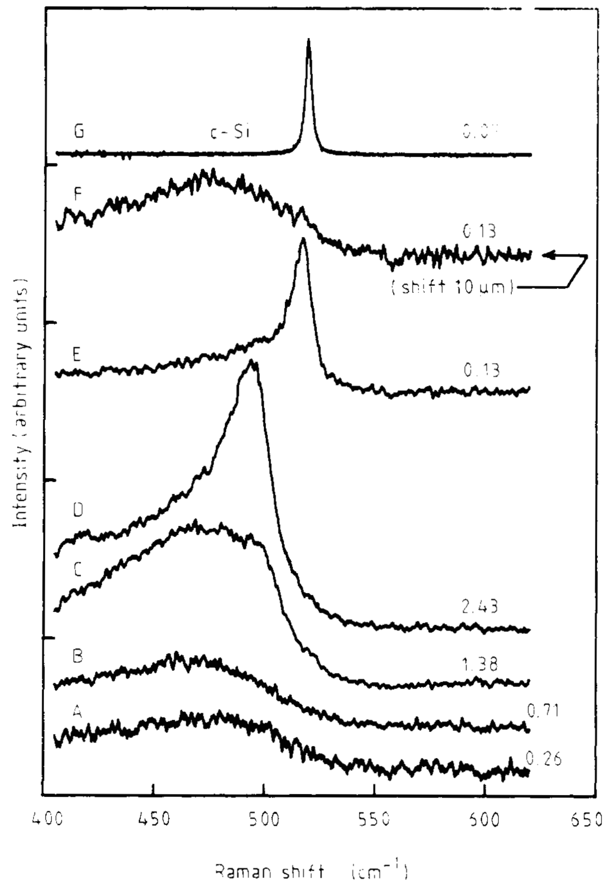

Figure 1. The Raman spectra of c-Si (curve G) and a-Si film (thickness 1.2 μm) probed by a 488 nm laser under various powers. The Raman intensity increases with the probe power. Its heating effect is observable in the graphs. For comparison, different magnification power is used for each spectrum. A, (×2); C, (×0.5); D, (×0.5); F, (×2); G, (×0.07).

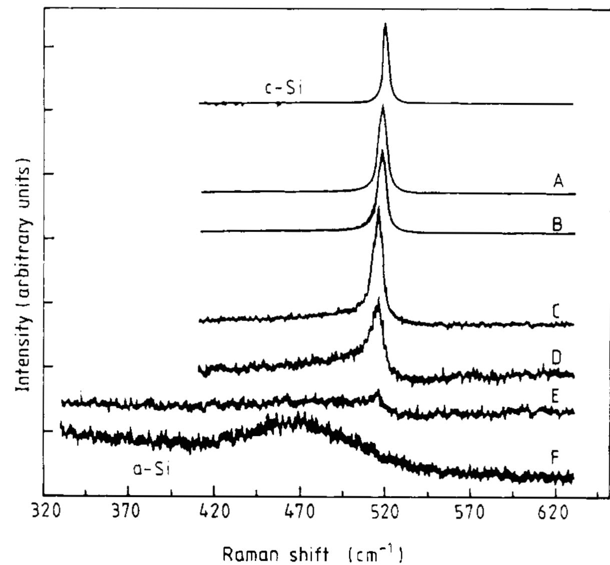

Figure 2. The Raman spectra of c-Si and a-Si film (thickness 1.2 μm) probed by a 488 nm laser of power ≤ 0.05 mW μm^{-2} after various fluences and at different magnifications: A, 1.1 J cm^{-2}, (×0.5); B, 0.38 J cm^{-2}; C, 0.3 J cm^{-2}, (×10); D, 0.16 J cm^{-2}, (×20); E, 0.1 J cm^{-2}, (×20); F, (×200).

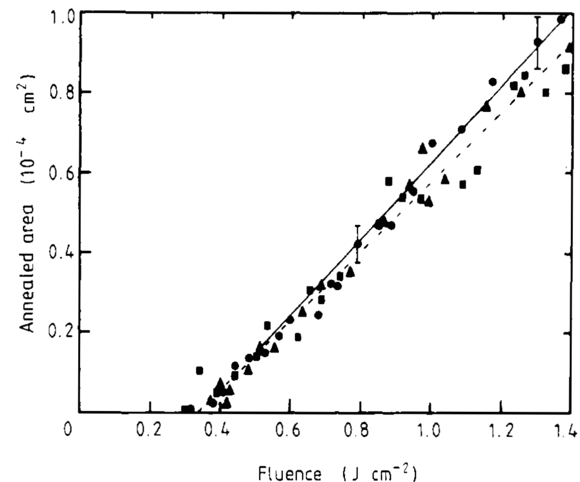

Figure 3. Graph showing the annealed area is proportional to excitation fluence for three film thicknesses ●, 0.8; ▲, 1.2; ■ 1.8 μm.

3. Results and discussion

3.1. Probe heating effect

The Raman spectra of c-Si and as-deposited a-Si are obtained by a 488 nm probe (figure 1). The sharp peak at 520 cm^{-1} of c-Si (figure 1, curve G) versus the broad feature (~60 cm^{-1}) around 475 cm^{-1} of as-deposited a-Si (figure 1, curve A) are used to distinguish between the crystalline and the amorphous structure. To ascertain the presence of any undesirable heating from the microprobe itself, we examined the heating effect of the probe by gradually increasing its power density (figure 1, curves A–D). From the spectra of the a-Si film, we find that the amorphous structure remains unchanged until its power density is 1.38 mW μm^{-2}, and a recrystallised peak starts to appear when its power density reaches 2.43 mW μm^{-2}. Comparing curve D with curve G of figure 1, the Raman peak shifts to a lower position and the width is greater. The lattice temperature can be estimated from this shift, which is 900–1100 °C [13] for the 2.43 mW μm^{-2} probe. We use a low-power probe to eliminate its heating effect.

For testing the spatial resolution of our microprobe, we used a lower-power probe (0.13 mW μm^{-2}) to measure the Raman spectrum of the film, which was annealed by the 2.34 mW μm^{-2} probe. The recrystallised peak was observed (figure 1, curve E) yet this peak disappeared when the sample was translated by a distance as small as 10 μm (figure 1, curve F). Therefore, the annealed region is less than 10 μm in diameter, which corresponds to the spot size of the probe. This confirms that the microprobe can be used to position the microstructure, and determine whether it is crystalline or amorphous.

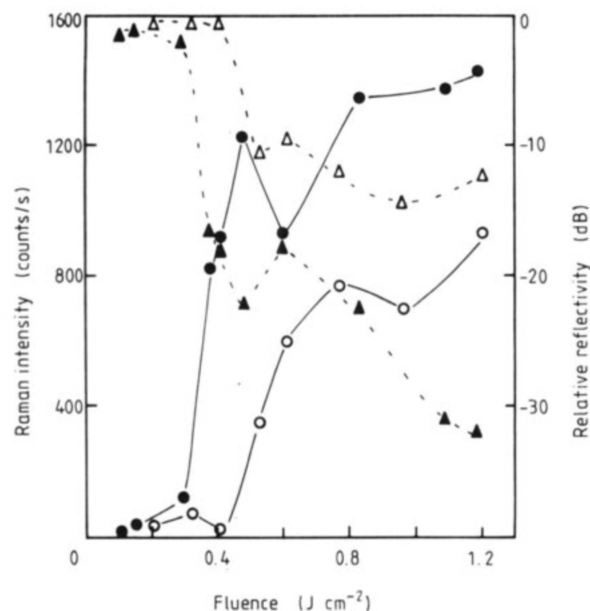

Figure 4. The annealed Raman intensity against fluence (○, 337 nm; ●, 580 nm) and the relative reflectivity against fluence (△, 337 nm; ▲, 580 nm). Both signals coincide at the transition around 0.6 and 0.4 J cm^{-2}.

3.2. Excitation effect

For eliminating the heating effect from the probe, a low-power probe (0.05 mW μm^{-2}) is used to measure the Raman spectrum of a-Si films under various fluences (figure 2). When the fluence is greater than 0.1 J cm^{-2} the recrystallised peak begins to emerge at 513 cm^{-1}, and moves gradually toward 518 cm^{-1} as the fluence increases. When the fluence reaches 0.38 J cm^{-2}, the Raman spectrum becomes similar to that of c-Si. Thus, the higher the excitation, the more the a-Si is recrystallised in the film. Three samples of different thicknesses are measured for examining the thickness effect. We find the annealed area is proportional to the fluence (figure 3) and their threshold fluences are more or less the same.

The excitation effects of both visible (580 nm) and ultraviolet (337 nm) wavelengths were investigated. For comparison, their Raman peak intensities and their relative reflectivities at the annealed centres are plotted against the applied fluence (figure 4). Below 0.3 J cm^{-2}, both films are only partially annealed on the top layer and the Raman intensities are low. Above 0.6 J cm^{-2}, which is well above the threshold of annealing, the intensities are high. In between, the Raman signal sharply rises around 0.4 J cm^{-2} for the dye laser but 0.6 J cm^{-2} for the N_2 laser. This apparent difference in transition is because the imaginary refractive index of the a-Si is much larger in UV than it is in the visible region. The measured reflectivity is 45% at 337 nm and 30% at 580 nm. Thus, their actual transitions should be closer to each other than what has been observed in the measurement. Just above these fluences, both Raman signals and the relative reflectivities show a dip followed by a plateau (figure 4). A similar dip feature was observed previously in the contrast transmission of an annealed Si film by argon laser [6], and this may be attributed to the competition between recrystallisation and quenching of the molten silicon.

3.3. Raman and optical correlation

As well as Raman signals, optical properties of the recrystallised film also reveal the annealing effect in annular band form after 1.1 J cm^{-2}. Both the reflection and the transmission micrographs (×400) of the annealed film (figures 5(*a*) and (*b*)) consist of three circumscribed regions which resemble the laser energy

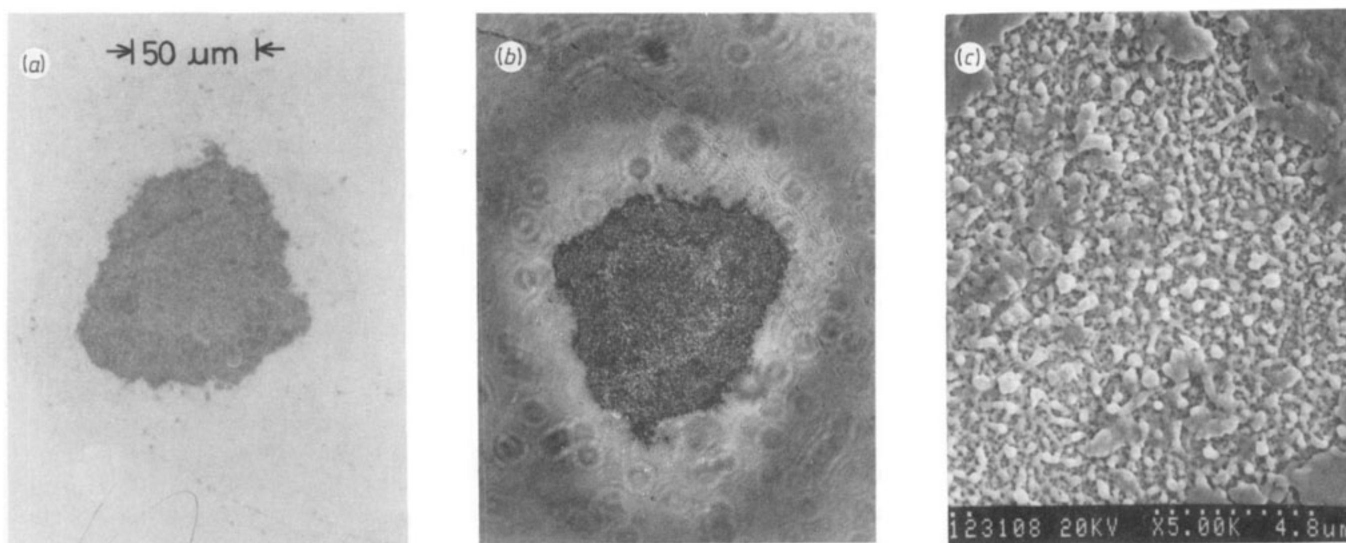

Figure 5. (*a*) Reflection and (*b*) transmission micrographs (×335). (*c*) SEM (×4062) picture of a-Si film excited by a 1.1 J cm^{-2}, 580 nm dye laser.

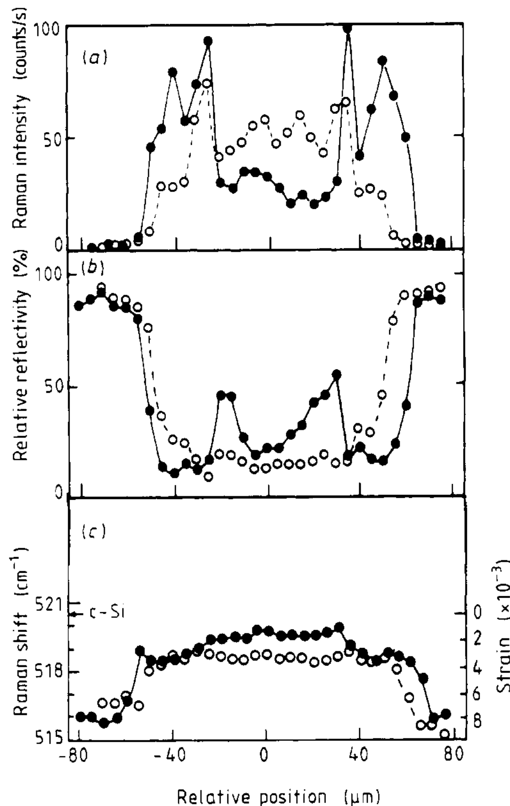

Figure 6. Horizontally scanned (*a*) Raman intensity, (*b*) reflectivity, and (*c*) Raman shift (i.e. strain) under one shot (○) and two shots (●) of 1.1 J cm^{-2}. All show clear boundaries; the Raman intensity and the reflectivity vary inversely.

profile. The number of bands increases with the laser fluence.

The SEM picture (figure 5(*c*)) reveals the annealed structure in more detail. There are many tiny crystals of various sizes in a porous network. The real causes of the network formation are not known yet but this may be ascribed to explosive crystallisation and its generated shock wave [8–11]. Because short-pulse excitation generates fast heating and cooling, the induced shock wave may propagate through the rapidly melted Si and cause it to compress and relax. It has been shown that surface ripples can be induced by this shock wave [14]. Consequently, some of the material is pushed outward and nucleates at the cool edges. Furthermore, because the substrate is not a single crystal, the annular pattern is formed in a mixed form of crystalline/amorphous structure, which can explain the Raman enhancement [15] of the annealed film.

The spatial profiles of the annealed film were measured by a weak 514.5 nm probe to examine the correlation between its Raman intensity and optical signal. Both measurements consist of three regions across the excited spot (figures 6(*a*) and (*b*)). The relative reflectivity of the central area (60 μm in diameter) is only 5–10% of the unexcited film, which corresponds to the same region of high Raman intensity. The narrow plateau (~5 μm) outside the central region, which corresponds to the first ring of its micrograph, is also observed in both measurements. Because the stability of the probe power is better than 1%, all irregular observations are completely due to the excited profile. Therefore, both the sharply varied reflectivity and Raman intensity can be used to locate the excited boundary. From all these measurements, one can notice two interesting features in the phase variation. One is that the spatial profile of the Raman intensity closely matches that of the optical micrograph; the other is the inverse relationship between the Raman intensity and the reflectivity, i.e. strong Raman signals are associated with poor reflection and vice versa.

3.4. Strain analysis

The asymmetric Raman lineshape is observable in figure 2, and this indicates that the strain variation does exist inside the probe region. It is known that the phonon frequency depends upon the temperature and the stress in the probed region. If one keeps the probe power below 0.05 mW μm^{-2}, the heating effect from the probe itself can be neglected and the Raman shift is only associated with the laser-induced stress τ which is given as [16]

$$\tau = \frac{3\omega_0 \Delta\Omega}{(S_{11} + 2S_{12})(p + 2q)}$$

where S_{11} and S_{12} are compliance coefficients, p and q are the deformation potential parameters. ω_0 is the phonon frequency and $\Delta\Omega$ is the Raman shift difference. The hydrostatic strain inside the annealed microstructure can be expressed as

$$\sigma_h = (S_{11} + S_{12})\tau = -1.735 \times 10^{-3}\Delta\Omega.$$

To achieve 0.65 cm^{-1} spectral resolution, 514.5 nm laser line and a 75 μm slit were used. The laser-induced tensile strain was then evaluated from the Raman shift as shown in figure 6(*c*). Because the pulse energy is large enough to recrystallise the a-Si but its cool edges can prevent the annealing process, the strain variation inside the annealed region is nearly uniform and is very large around its edges.

3.5. Recrystallisation to amorphisation transition

The Raman peak intensity is more sensitive to the structure than the Raman shift so the details of annealed structure are analysed in terms of intensity. As one anticipates, the amorphisation of silicon not only requires sufficient energy to reach its melting point but it also needs extremely rapid cooling to freeze the random structure. According to the interpretation of Cullis *et al* [11], a solidification velocity greater than 15 m s^{-1} may account for the amorphised silicon. Wood and Geist [17] propose that a supercooling rate $> 4 \times 10^{10}$ °C s^{-1} is needed to suppress nucleation. For fitting the Raman lineshape, Compaan *et al* [18] assumed the cooling rate to be 8×10^{10} °C s^{-1} during the pulsed laser annealing in Si. Considering such a

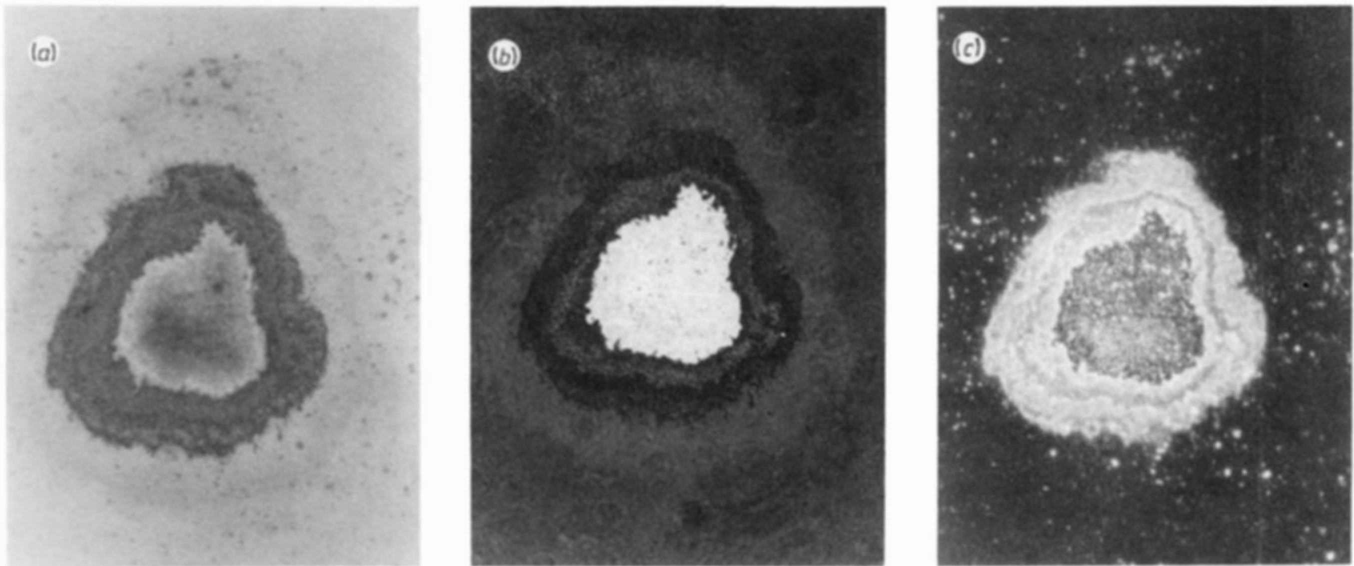

Figure 7. (*a*) and (*b*) are the same as in figures 5(*a*) and (*b*) after two shots of 1.1 J cm^{-2}. (*c*) phase contrast picture of (*a*).

cooling rate in a 0.2 μm molten layer, one can obtain the solidification velocity of about 20 m s^{-1}. Thus, we believe that a 600 ps laser pulse can achieve these conditions and amorphise the annealed Si film.

The fluence control is critical for re-amorphising the annealed film. In fact, drastic changes in the Raman intensity and the reflection resulting from further annealing and quenching (double shots) are observed (figures 7(*a*) and (*b*)). After a consecutive pulse, all the micrographs have the similar annular pattern except a much brighter centre and broadened dark rings. The pattern and the boundary features can be seen more clearly in the phase contrast picture (figure 7(*c*)). Letting the *x* and *y* axes denote the first and the second laser fluences respectively, we plot the contrast transmission (CT) and reflection (CR) with respect to the

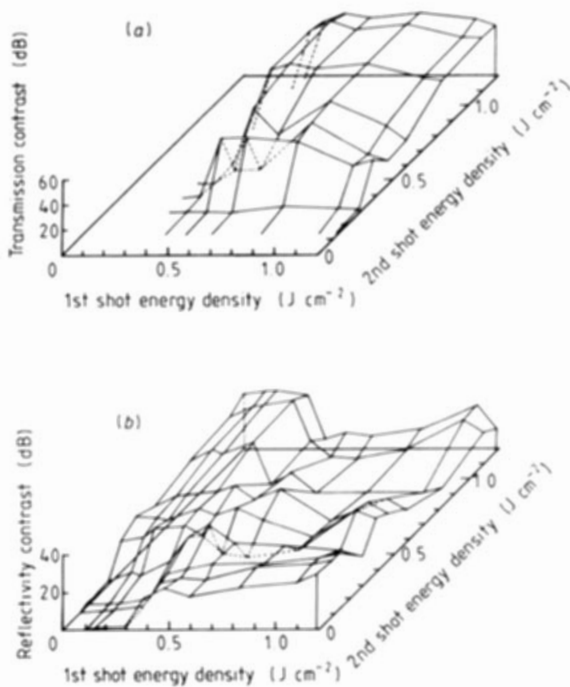

Figure 8. (*a*) Transmission and (*b*) reflectivity contrasts with respect to the fresh film against the first and the second fluence. Its feasibility for erasable recording is also indicated on these graphs.

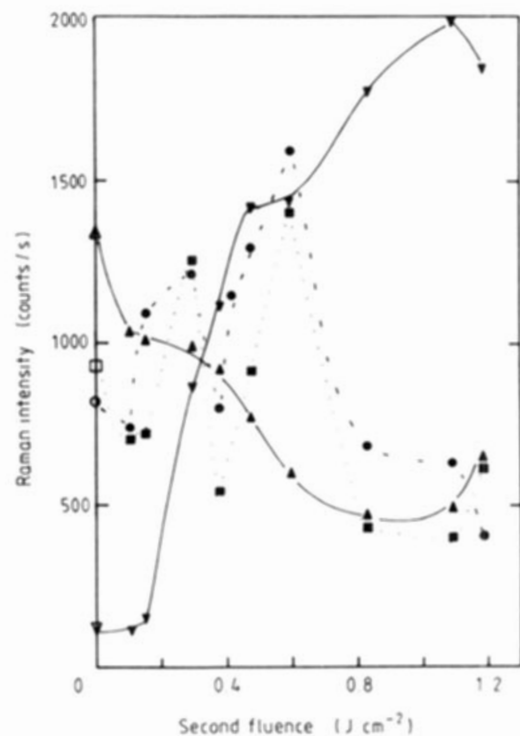

Figure 9. The Raman intensity against the second fluence (▲ ● ■ ▼) after different first shots (▲, 0.83; ●, 0.38; ■, 0.59; ▼, 0.29 J cm^{-2}). The intensity variation critically depends on both fluences. The film is 1.2 μm thick.

fresh film along the z axis (figures 8(a) and (b)). All these valleys, ridges, plateaus and basins in these contrast plots are useful for understanding the erasability of the film since all the optical signals can be dramatically changed by an appropriate fluence.

Analysing the Raman intensity under various second fluences (figure 9) we can categorise it into three regimes. The first regime is that the first fluence is low, i.e. less than 0.3 J cm^{-2}, which only gives a weak Raman signal (below 120 counts/s); when the second excitation is high (larger than 0.4 J cm^{-2}) the Raman intensity suddenly increases drastically. This is because the first pulse only forms some microcrystals which can act as the nucleation centre for more recrystallisation by an extra shot. The second regime covers the first fluence between 0.3 and 0.6 J cm^{-2}, which also produces a median Raman intensity between 500 and 1000 counts/s. The extra shot can either increase or reduce the Raman intensity. Since both crystalline and amorphous Si exist near the transition, the extra energy can dramatically change the annealed structure. Thus, the final Raman intensity after a consecutive excitation can exhibit a large variation. The final regime is that the first fluence is high, i.e. larger than 0.6 J cm^{-2}, which gives a strong Raman signal (above 1200 counts/s) and then the extra shot reduces the Raman intensity and increases the transmission in the central region. We also notice that the scattering intensity around the edge is twice that in the centre. This indicates there is more recrystallised material around the edge than in the centre. A similar feature was also observed by Nissim *et al* [19] on ion-implanted Si wafer. In our stress analysis the structure around the edge is a mixture of amorphous and crystalline Si, so that some of the amorphous Si around the edge is recrystallised by the second shot.

4. Conclusion

From these microprobe Raman and optical measurements on the a-Si film excited with a picosecond laser, one can notice that the laser-induced phase change is accompanied with large optical contrasts and is reversible (annealing and quenching), so it could be used for erasable optical recording. The transition thresholds for visible and UV excitations are close to each other.

Acknowledgments

We are grateful to Professor M C Chen for his valuable suggestions. We also wish to thank Mr S Y Wu for his technical help in taking the SEM pictures. The financial support from the National Science Council of the Republic of China (NSC78-0208-M009-25) is gratefully acknowledged.

References

[1] Lee C (ed) 1984 *Picosecond Optoelectronic Devices* (New York: Academic) ch 4 pp 100–3, and references therein

[2] Joannopoulous J D and Lucovsky G (ed) 1984 *The Physics of Hydrogenated Amorphous Silicon I* (*Springer Topics in Applied Physics* **55**) (Berlin: Springer) ch 3, 6

[3] Madan A, Thompson M, Adler D and Hamakawa Y (eds) 1987 *Amorphous Silicon Semiconductors—Pure and Hydrogenated (Mater. Res. Soc. Proc. 95)* (Pittsburgh: Material Research Society)

[4] Bohm M 1988 *Solid State Technol.* September 125

[5] Janai M and Moser F 1982 *J. Appl. Phys.* **53** 1385

[6] Lee M C, Tseng C J, Huang C R and Huang T H 1987 *Japan. J. Appl. Phys.* **26** 193

[7] Lee M C, Huang C R and Lin C C 1987 *Proc. Int. Symp. on Optical Memory* (*Tokyo*) *1987 Japan. J. Appl. Phys.* **26** Suppl. **26–4** 67

[8] Thompson M O, Galvin G J, Mayer J W, Peercy P S, Poate J M, Jacobson D C, Cullis A G and Chew N G 1984 *Phys. Rev. Lett.* **52** 2360

[9] Kanemitsu Y, Kuroda H and Nakada I 1986 *Japan. J. Appl. Phys.* **25** 1377

[10] Bruines J J P, van Hal R P M, Koek B H, Viegers M P A and Boots H M J 1987 *Appl. Phys. Lett.* **50** 507

[11] Cullis A G, Webber H C, Chew N G, Poate J M and Baeri P 1982 *Phys. Rev. Lett.* **49** 219

[12] Lyon S A, Nemanich R J, Johnson N M and Biegelsen D K 1982 *Appl. Phys. Lett.* **40** 316

[13] Balkanski M, Wallis R F and Haro E 1983 *Phys. Rev.* B **28** 1928

[14] Young J F, Sipe J E and van Driel H M 1984 *Phys. Rev.* B **30** 2001

[15] Lee M C, Huang C R, Chang Y S and Chao Y F 1989 *Phys. Rev.* B **40** 10420

[16] Lee M C 1986 *Chin. J. Phys.* **24** 69

[17] Wood R F and Geist G A 1986 *Phys. Rev.* B **34** 2606

[18] Compaan A, Lee M C and Trott G J 1985 *Phys. Rev.* B **32** 6731

[19] Nissim Y I, Sapriel J and Oudar J L 1983 *Appl. Phys. Lett.* **42** 504